Asteroid photometry

ASTEROIDS IV p129 – 150

J.Y. Li et al., 2015.

20243069 M1 土井知也

Contents

1.1. Importance of planetary photometry

・測光に関わる幾何学的な用語の定義

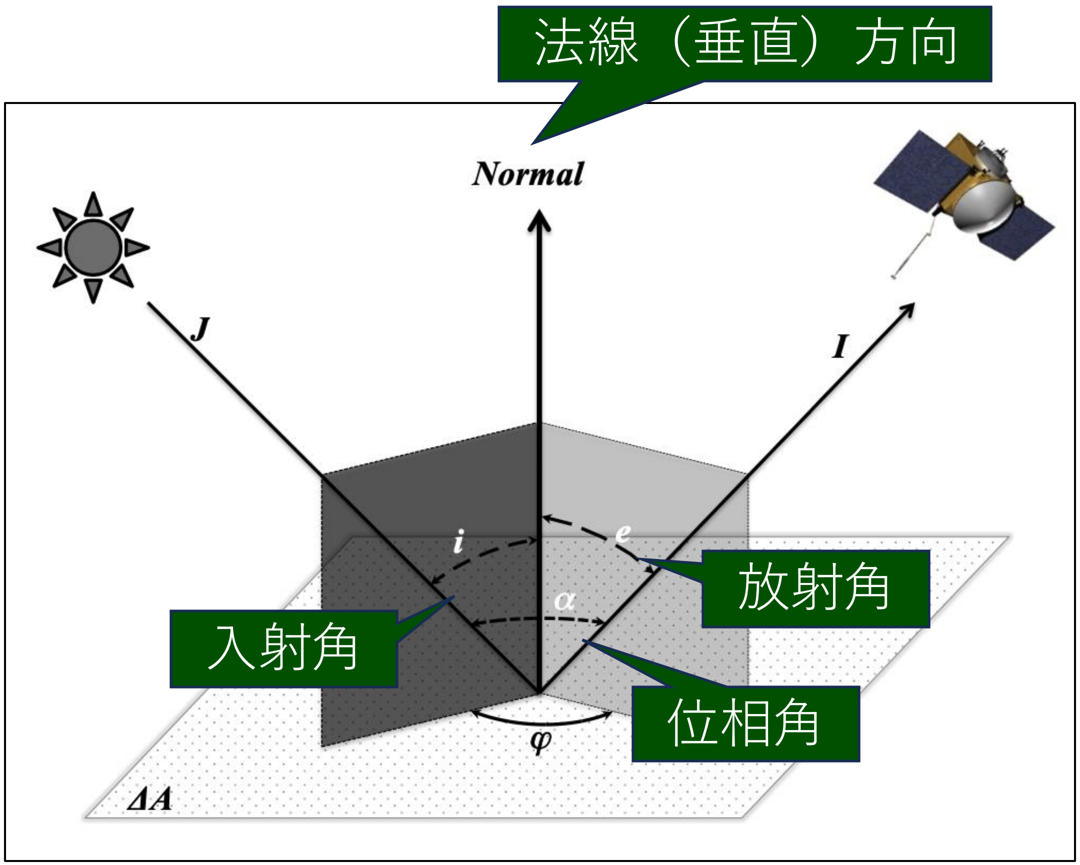

Fig. 1. Schematic diagram of bidirectional reflectance from a surface element ΔA, showing the various angles.

1.1. Importance of planetary photometry

小惑星は点光源！
かつ、観測中に自転
してしまう！

・小惑星の測光観測で分かる物理量
<u>表面特性、特に表面組成</u>
→全反射面（表と裏）を完全にパラメータ化できない
　・粒子サイズ　・屈折率
　・空隙率　　　・ラフネス　に依存するが、、、
・フェイズレッドニング
一般に位相角が大きくなるほど表面スペクトルが赤く
実験室での結果と比較するために補正が必要
（入射角, 放射角, 位相角＝0°, 0°, 0°）
・探査機の”その場”観測前に地上測光データを利用

1.2. Scope of this chapter

最初の”その場“観測前には形状が分かっていなかったのでメインの研究対象

・太陽位相角に依存し明るさが減光
　暗い天体はより急激に減光
　→<u>位相関数</u>
　　多重散乱？
　　表面のラフネスさ？
　　（特に40°以上）

・測光的特徴と偏光的
　特徴に相関がある

モデルフィット

実際の観測データ

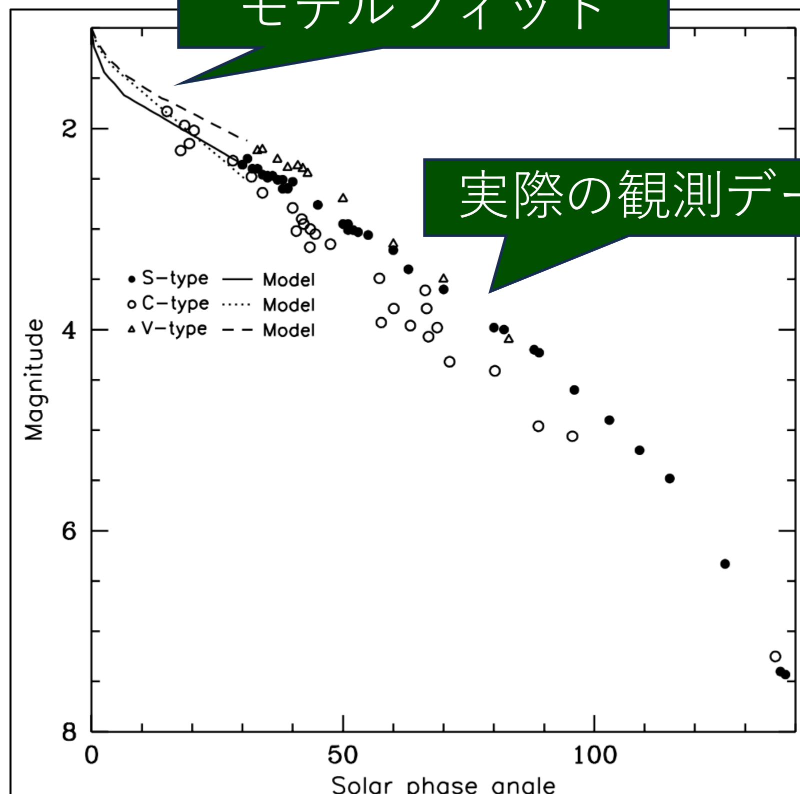

Fig. 2. The phase functions of three asteroid classes, all normalized at zero degree phase angle.

2.1. Basic Concepts

・いくつかの<u>反射率</u>と<u>アルベド</u>の定義

反射率：散乱された輝度と入射照度の比

アルベド：全入射光を等方的に散乱する理想面のとき

ランバート面

Table 1 The definitions of some commonly used reflectance quantities

Quantity	Definition	Formula	Ref [*]
Bidirectional reflectance	Ratio of the scattered radiance towards (i, e, α) to the collimated incident irradiance	$r(i, e, \alpha) = I(i, e, \alpha)/J$ [ster^{-1}]	pp195
Bidirectional reflectance distribution function (BRDF)	Ratio of the scattered radiance towards (i, e, α) to the collimated power incident on a unit area of the surface	BRDF = $I(i, e, \alpha)/J\mu_0 = r/\mu_0$ [ster^{-1}]	pp 263
Radiance factor (RADF)	Ratio of the bidirectional reflectance of a surface to that of a perfectly scattering surface[$] illuminated at normal direction	RADF = $\pi r(i, e, \alpha)$ = [I/F]	pp 264
Reflectance factor (or reflectance coefficient, REFF)	Ratio of the reflectance of a surface to that of a perfectly diffused surface under the same conditions of illumination and viewing	REFF = $\pi r/\mu_0$ = [I/F]/μ_0	pp 263
Lambertian albedo	Ratio of the total scattered irradiance towards all directions from a Lambert surface to incident power per unit area	$A_L = P_L/J\mu_0$ Perfectly scattering surface has $A_L = 1$	pp. 187
Normal albedo	Ratio of the reflectance of a surface observed at zero phase angle from an arbitrary direction to that of a perfectly diffuse surface located at the same position, but illuminated and observed perpendicularly	$A_n = \pi r(e, e, 0)$	pp 296
Geometric albedo (physical albedo)	Ratio of the integral brightness of a body at zero phase angle to the brightness of a perfect Lambert disk of the same size and at the same distance, but illuminated and observed perpendicularly. It is the weighted average of the normal albedo over the illuminated area of the body	$A_p = \int_{2\pi} r(e, e, 0)\mu\, d\Omega$ [#]	pp. 298
Bond albedo (spherical albedo, or global albedo)	Total fraction of incident irradiance scattered by a body into all directions	$A_s = \frac{1}{\pi}\int_{2\pi}\int_{2\pi} r(i, e, \alpha)\mu\, d\Omega_e\, d\Omega_i$	pp. 301
Bolometric albedo (radiometric albedo)	Average of the spectral albedo $A_s(\lambda)$ weighted by the spectral irradiance of the Sun $J_s(\lambda)$	$A_b = \frac{\int_0^\infty A_S(\lambda) J_S(\lambda)\, d\lambda}{\int_0^\infty J_S(\lambda)\, d\lambda}$	pp. 302
Phase integral		$q = 2\int_0^\pi \Phi_p(\alpha) \sin\alpha\, d\alpha$	pp. 302

2.1. Basic Concepts

- 幾何（ジオメトリック）アルベド
  各位相角での明るさ　幾何アルベド×位相関数
  計算上1を越えることも　例）エンケラドス　1.38

Table 1 The definitions of some commonly used reflectance quantities

Quantity	Definition	Formula	Ref *
Bidirectional reflectance	Ratio of the scattered radiance towards (i, e, α) to the collimated incident irradiance	$r(i, e, \alpha) = I(i, e, \alpha)/J$ [ster^{-1}]	pp195
Bidirectional reflectance distribution function (BRDF)	Ratio of the scattered radiance towards (i, e, α) to the collimated power incident on a unit area of the surface	BRDF = $I(i, e, \alpha)/J\mu_0 = r/\mu_0$ [ster^{-1}]	pp 263
Radiance factor (RADF)	Ratio of the bidirectional reflectance of a surface to that of a perfectly scattering surface$^{\$}$ illuminated at normal direction	RADF = $\pi r(i, e, \alpha)$ = [I/F]	pp 264
Reflectance factor (or reflectance coefficient, REFF)	Ratio of the reflectance of a surface to that of a perfectly diffused surface under the same conditions of illumination and viewing	REFF = $\pi r/\mu_0$ = [I/F]/μ_0	pp 263
Lambertian albedo	Ratio of the total scattered irradiance towards all directions from a Lambert surface to incident power per unit area	$A_L = P_L/J\mu_0$ Perfectly scattering surface has $A_L = 1$	pp. 187
Normal albedo	Ratio of the reflectance of a surface observed at zero phase angle from an arbitrary direction to that of a perfectly diffuse surface located at the same position, but illuminated and observed perpendicularly	$A_n = \pi r(e, e, 0)$	pp 296
Geometric albedo (physical albedo)	Ratio of the integral brightness of a body at zero phase angle to the brightness of a perfect Lambert disk of the same size and at the same distance, but illuminated and observed perpendicularly. It is the weighted average of the normal albedo over the illuminated area of the body	$A_p = \int_{2\pi} r(e, e, 0)\mu \, d\Omega$ #	pp. 298
Bond albedo (spherical albedo, or global albedo)	Total fraction of incident irradiance scattered by a body into all directions	$A_s = \frac{1}{\pi}\int_{2\pi}\int_{2\pi} r(i, e, \alpha)\mu \, d\Omega_e \, d\Omega_i$	pp. 301
Bolometric albedo (radiometric albedo)	Average of the spectral albedo $A_s(\lambda)$ weighted by the spectral irradiance of the Sun $J_s(\lambda)$	$A_b = \frac{\int_0^\infty A_S(\lambda) J_S(\lambda)\, d\lambda}{\int_0^\infty J_S(\lambda)\, d\lambda}$	pp. 302
Phase integral		$q = 2\int_0^\pi \Phi_p(\alpha) \sin\alpha \, d\alpha$	pp. 302

2.1. Basic Concepts

- ボンドアルベド　1を越えることはない

  小惑星では、Vバンドのボンドアルベドが

  ボロメトリックアルベドの近似として利用

Table 1 The definitions of some commonly used reflectance quantities

Quantity	Definition	Formula	Ref *
Bidirectional reflectance	Ratio of the scattered radiance towards (i, e, α) to the collimated incident irradiance	$r(i,e,\alpha) = I(i,e,\alpha)/J$ [ster^{-1}]	pp195
Bidirectional reflectance distribution function (BRDF)	Ratio of the scattered radiance towards (i, e, α) to the collimated power incident on a unit area of the surface	BRDF = $I(i,e,\alpha)/J\mu_0 = r/\mu_0$ [ster^{-1}]	pp 263
Radiance factor (RADF)	Ratio of the bidirectional reflectance of a surface to that of a perfectly scattering surface$ illuminated at normal direction	RADF = $\pi r(i,e,\alpha)$ = [I/F]	pp 264
Reflectance factor (or reflectance coefficient, REFF)	Ratio of the reflectance of a surface to that of a perfectly diffused surface under the same conditions of illumination and viewing	REFF = $\pi r/\mu_0$ = [I/F]/μ_0	pp 263
Lambertian albedo	Ratio of the total scattered irradiance towards all directions from a Lambert surface to incident power per unit area	$A_L = P_L/J\mu_0$ Perfectly scattering surface has $A_L = 1$	pp. 187
Normal albedo	Ratio of the reflectance of a surface observed at zero phase angle from an arbitrary direction to that of a perfectly diffuse surface located at the same position, but illuminated and observed perpendicularly	$A_n = \pi r(e,e,0)$	pp 296
Geometric albedo (physical albedo)	Ratio of the integral brightness of a body at zero phase angle to the brightness of a perfect Lambert disk of the same size and at the same distance, but illuminated and observed perpendicularly. It is the weighted average of the normal albedo over the illuminated area of the body	$A_p = \int_{2\pi} r(e,e,0)\mu\, d\Omega$ #	pp. 298
Bond albedo (spherical albedo, or global albedo)	Total fraction of incident irradiance scattered by a body into all directions	$A_s = \frac{1}{\pi}\int_{2\pi}\int_{2\pi} r(i,e,\alpha)\mu\, d\Omega_e\, d\Omega_i$	pp. 301
Bolometric albedo (radiometric albedo)	Average of the spectral albedo $A_s(\lambda)$ weighted by the spectral irradiance of the Sun $J_s(\lambda)$	$A_b = \frac{\int_0^\infty A_S(\lambda) J_S(\lambda)\, d\lambda}{\int_0^\infty J_S(\lambda)\, d\lambda}$	pp. 302
Phase integral		$q = 2\int_0^\pi \Phi_p(\alpha) \sin\alpha\, d\alpha$	pp. 302

2.2. Empirical models

- 探査機による（表面空間）分解測光モデルでの反射率
  幾何アルベドが ~1：Lambertモデル
  < 0.2のC-, D-, P-type：Lommel-Seeligerモデル
  S-, V-, E-type：Lunar-Lambertモデル

Table 2 Commonly used empirical photometric models

Model	RADF*	Normal Albedo (A_n)	Geometric Albedo (A_p)	Reference
Lambert	$A_L\mu_o f(\alpha)$	$A_L f(0)$	$\frac{2}{3}A_L f(0)$	
Lommel-Seeliger	$A_{LS}\frac{\mu_o}{\mu_o+\mu}f(\alpha)$	$\frac{1}{2}A_{LS}f(0)$	$\frac{1}{2}A_{LS}\ f(0)$	
Lunar-Lambert	$A_{LL}\left[L(\alpha)\frac{2\mu_0}{\mu_0+\mu}+(1-L(\alpha))\mu_0\right]f(\alpha)$ $ $L(\alpha)=1+A_1\alpha+A_2\alpha^2+A_3\alpha^3$	$A_{LL}f(0)$	$\frac{2+L(0)}{3}A_{LL}f(0)$	McEwen (1991; 1996)
Minnaert	$A_M\mu_o^{k(\alpha)}\ \mu^{k(\alpha)-1}f(\alpha)$ $k(\alpha)=k_0+b\alpha$ #	$A_M f(0)$	$\frac{2}{2k+1}\ A_M f(0)$	Minnaert (1941) Li et al. (2009; 2013b)
Akimov	$A_n\cos\frac{\alpha}{2}\cos\left(\frac{\pi}{\pi-\alpha}\left(\Lambda-\frac{\alpha}{2}\right)\right)\frac{\cos^{\frac{\alpha}{\pi-\alpha}}\beta}{\cos\Lambda}f(\alpha)$	$A_n f(0)$	$A_n f(0)$	Shkuratov et al. (2011)

* $f(\alpha)$ is a surface phase function, generally normalized to unity at zero phase angle. A with various subscriptions are constants that are directly proportional to the normal albedo and geometric albedo of the surface. Therefore, the RADF can also be expressed in terms of normal albedo or geometric albedo.
$ L(α) is a partition parameter between the LS term and the Lambert term. It usually depends on phase angle.
\# This is an empirical model of $k(\alpha)$ as adopted by Li et al. (2009; 2013a). Masoumzadeh et al. (2014) show, from their work on asteroid Lutetia using Rosetta flyby data, that the phase angle dependence of k might be better described with a 2nd order polynomial.

2.2. Empirical models

- 表面位相関数（経験式）
  どれもf(0)=1

Fig. 2. The phase functions of three asteroid classes, all normalized at zero degree phase angle.

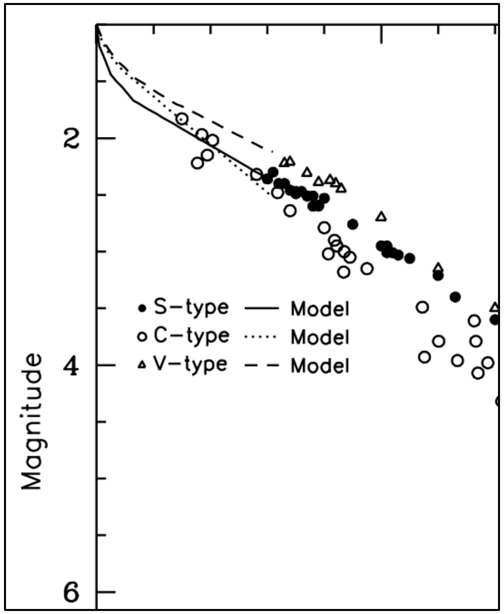

Table 3 List of empirical surface phase functions

Model	Empirical Phase Function	References
Exponential	$f(\alpha) = e^{\beta\alpha+\gamma\alpha^2+\delta\alpha^3}$	Takir et al. (2014)
Linear-magnitude	$f(\alpha) = 10^{-0.4\beta\alpha}$	Li et al. (2009; 2013a)
Polynomial-magnitude	$f(\alpha) = 10^{-0.4(\beta\alpha+\gamma\alpha^2+\delta\alpha^3)}$	Takir et al. (2014)
Lunar/ROLO	$f(\alpha) = C_0e^{-C_1\alpha} + A_0 + A_1\alpha + A_2\alpha^2 + A_3\alpha^3 + A_4\alpha^4$	Hillier et al. (1999); Buratti et al. (2011)
Linear-Exponential	$f(\alpha) = ae^{-\alpha/d} + b + k\alpha$	Piironen, 1994; Kaasalainen et al. (2001; 2003)
Akimov	$f(\alpha) = \frac{e^{-\mu_1\alpha}+me^{-\mu_2\alpha}}{1+m}$ *	Akimov (1988)

* μ_1 and μ_2 are model parameters, not to be confused with μ_0 and μ, which are the cosines of incidence angle and emission angle, respectively.

2.3. Physically Motivated Models

- 物理的特性を用いた解析的な測光モデル

  1. アルベド、平均サイズのレゴリス粒子の単一散乱
  2. 多重散乱
  3. マクロ的な表面テクスチャの影響
  4. 衝効果（位相角0°付近で急増光）

  の要素が複雑に相互作用

- Hapkeモデル　→　最も一般的
- Shkuratovモデル
- Lumme-Bowellモデル

2.3. Physically Motivated Models

・Hapkeモデルでの反射率(輝度因子：RADF)

$$R(\mu_0, \mu, \alpha) = K \frac{\varpi_0}{4} \frac{\mu_0'}{\mu_0' + \mu'} \left[(1 + B_{SH}(\alpha)) P(\alpha) + M\left(\frac{\mu_0'}{K}, \frac{\mu'}{K}, \alpha\right) \right] (1 + B_{CB}(\alpha)) S(\mu_0', \mu', \alpha)$$

Table 5 Particle single scattering phase functions

Name	Expression	Parameters	Reference
Modified Schoenberg	$P(\alpha) = [\sin\lvert\alpha\rvert + (\pi - \lvert\alpha\rvert)\cos(\lvert\alpha\rvert)/\pi + 0.1(1-\cos(\lvert\alpha\rvert))^2]$		Hapke (1963,1966)
Two-Parameter Legendre Polynomial (2PLP)	$P(\alpha) = 1 + b\cos(\alpha) + c\,(\frac{3}{2}\cos^2(\alpha) - \frac{1}{2})$	b,c	Hapke (1981)
One-Parameter Henyey-Greenstein (1PHG)	$P(a) = (1-g^2)/(1+2\,g\cos(a) + g^2)^{3/2}$	g	Buratti and Veverka (1983)
Two-Parameter Henyey-Greenstein (2PHG, form #1)	$P(\alpha) = \frac{(1+c)}{2} \frac{(1-b^2)}{(1-2b\cos(\alpha)+b^2)^{3/2}} + \frac{(1-c)}{2} \frac{(1-b^2)}{(1+2b\cos(\alpha)+b^2)^{3/2}}$	b,c	McGuire and Hapke (1995)
Two-Parameter Henyey-Greenstein (2PHG, form #2)	$P(\alpha) = (1-c)\frac{(1-b^2)}{(1+2b\cos(\alpha)+b^2)^{3/2}} + c\frac{(1-b^2)}{(1-2b\cos(\alpha)+b^2)^{3/2}}$	b,c	Hartman and Domingue (1998)
Three-Parameter Henyey-Greenstein (3PHG, form #1)	$P(\alpha) = (1-f)\frac{(1-g_1^2)}{(1+2g_1\cos(\alpha)+g_1^2)^{3/2}} + (f)\frac{(1-g_2^2)}{(1+2g_2\cos(\alpha)+g_2^2)^{3/2}}$	g_1,g_2,f	Helfenstein et al. (1991)
Three-Parameter Henyey-Greenstein (3PHG, form #2)	$P(\alpha) = (f)\frac{(1-g_1^2)}{(1+2g_1\cos(\alpha)+g_1^2)^{3/2}} + (1-f)\frac{(1-g_2^2)}{(1-2g_2\cos(\alpha)+g_2^2)^{3/2}}$	g_1,g_2,f	Deau and Helfenstein (2015)
Lumme-Bowell	$P(\alpha) = 0.95e^{-0.4\alpha} + 16.15\,e^{-4.0\alpha}$		Lumme and Bowell (1981b)

2.3. Physically Motivated Models

・P(α)：
平均粒子の単一散乱位相関数

衝効果

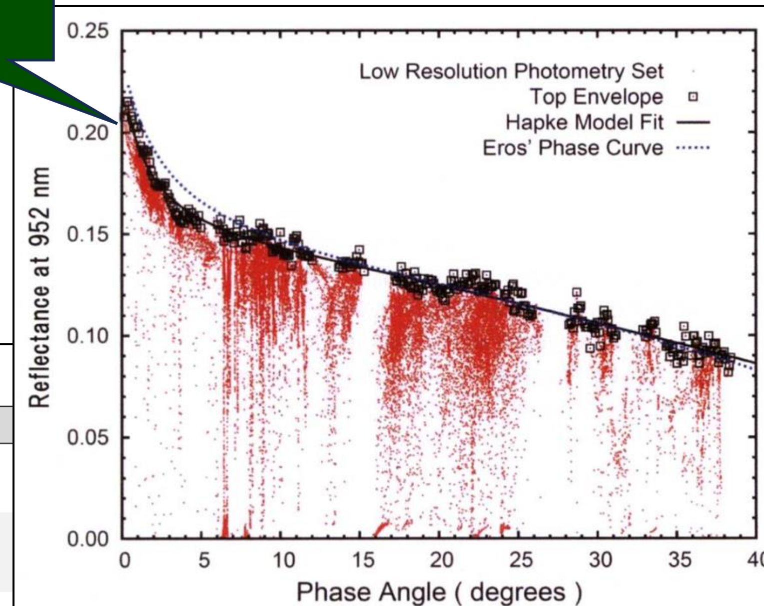

Fig. 3. Phase angle function of Itokawa.

Table 5 Particle single scattering phase functions

Name	Expression		
Modified Schoenberg	$P(\alpha) = [\sin\lvert\alpha\rvert + (\pi - \lvert\alpha\rvert)\cos(\lvert\alpha\rvert)/\pi + 0.1(1-\cos(\lvert\alpha\rvert))^2]$		
Two-Parameter Legendre Polynomial (2PLP)	$P(\alpha) = 1 + b\cos(\alpha) + c\left(\frac{3}{2}\cos^2(\alpha) - \frac{1}{2}\right)$		
One-Parameter Henyey-Greenstein (1PHG)	$P(a) = (1-g^2)/(1+2\,g\cos(a) + g^2)^{3/2}$		(1983)
Two-Parameter Henyey-Greenstein (2PHG, form #1)	$P(\alpha) = \frac{(1+c)}{2}\frac{(1-b^2)}{(1-2b\cos(\alpha)+b^2)^{3/2}} + \frac{(1-c)}{2}\frac{(1-b^2)}{(1+2b\cos(\alpha)+b^2)^{3/2}}$	b,c	McGuire and Hapke (1995)
Two-Parameter Henyey-Greenstein (2PHG, form #2)	$P(\alpha) = (1-c)\frac{(1-b^2)}{(1+2b\cos(\alpha)+b^2)^{3/2}} + c\frac{(1-b^2)}{(1-2b\cos(\alpha)+b^2)^{3/2}}$	b,c	Hartman and Domingue (1998)
Three-Parameter Henyey-Greenstein (3PHG, form #1)	$P(\alpha) = (1-f)\frac{(1-g_1^2)}{(1+2g_1\cos(\alpha)+g_1^2)^{3/2}} + (f)\frac{(1-g_2^2)}{(1+2g_2\cos(\alpha)+g_2^2)^{3/2}}$	g_1, g_2, f	Helfenstein et al. (1991)
Three-Parameter Henyey-Greenstein (3PHG, form #2)	$P(\alpha) = (f)\frac{(1-g_1^2)}{(1+2g_1\cos(\alpha)+g_1^2)^{3/2}} + (1-f)\frac{(1-g_2^2)}{(1-2g_2\cos(\alpha)+g_2^2)^{3/2}}$	g_1, g_2, f	Deau and Helfenstein (2015)
Lumme-Bowell	$P(\alpha) = 0.95e^{-0.4\alpha} + 16.15\,e^{-4.0\alpha}$		Lumme and Bowell (1981b)

2.3. Physically Motivated Models

・$1 + B_{SH}(\alpha)$：シャドーハイディング効果(SHOE)
衝の位置では背後からの光で自ら（観測機器）の影が
隠され増光→衝効果の要因の1つ

・ $1 + B_{CB}(\alpha)$：コヒーレント後方散乱効果(CBOE)
入射光と反対方向の散乱光が強くなり増光
→まだ理解が進んでいないが衝効果の要因の1つ

→大気がなく、レゴリスで覆われた天体表面で顕著
→小惑星（月）の測光観測において衝効果の影響は
大きい！

2.3. Physically Motivated Models

・Shkuratovモデルでの反射率（輝度因子：RADF）

$$R(\mu_o, \mu, \alpha) = A_n f_{SHOE}(\alpha)\, f_{CBOE}(\alpha)\, d(\Lambda, \beta, \alpha)$$

衝効果に
関わる項

・Lumme-Bowellモデル

$$\mathrm{V}(\alpha) = \mathrm{H} - 2.5\log_{10}[\mathrm{G}_1\Phi_1(\alpha) + \mathrm{G}_2\Phi_2(\alpha) + (1 - \mathrm{G}_1 - \mathrm{G}_2)\Phi_3(\alpha)]$$

→測光補正から小惑星の絶対等級(H)の導出が可能
（太陽、地球から1 auかつ位相角0°の明るさ）

→最も使われているのはHapkeモデル

2.4. Effects of Shape Models on Photometric Modeling

- 小惑星は不規則な形状→形状モデルが必要
  特に探査機によるサンプリングで非常に重要
- 小さな尾根やクレーターがローカルな表面輝度に
  与える影響を無視できない→大きな誤差に

Fig. 4. Shape image of Itokawa.

2.5. Testing of Physically-Motivated Models

・Hapkeモデルの検証、改良
フィッティング関数、パラメータ、誤差解析など
1. 実験室での研究
2. コンピュータモデリング
3. “その場”観測

最も貢献！

→単一散乱アルベド、ラフネスさ、空隙率といった
各測光パラメータの特性を一意に特定することは困難
・月レゴリスサイズと小惑星レゴリスのラフネスさ
・衝効果にCBOEとSHOEが寄与
・波長依存生について

3. OBSERVATIONAL DEVELOPMENTS

・探査機による”その場”観測以前は、
＜30° の点光源としての地上観測のみ

・探査機による調査で判明
1. 3次元形状の推定（非球体）
2. ローカルな輝度の変化（ラブルパイル）
3. 地形依存のアルベド、色の不均一（表と裏）

・イトカワは詳細に地表（表も裏も）を空間分解観測できた貴重な例
→フライバイでは不可能

3.1. Ceres

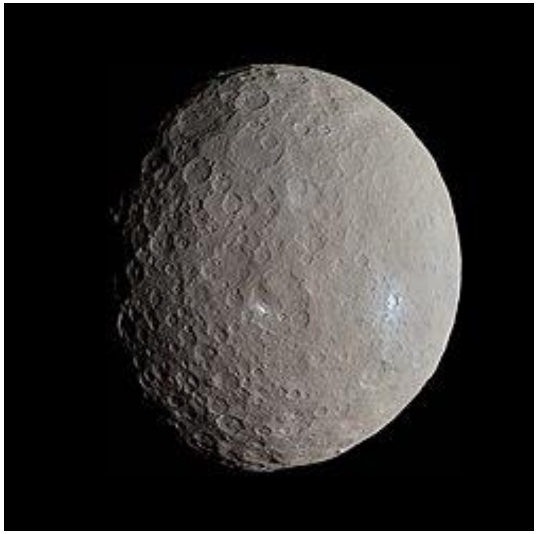

Fig. 5. Image of Ceres.

- 小惑星かつ準惑星（巨大）
  粗さパラメータが44°→非常に大きい
  表面組成、アルベドが全面的に非常に均一

Table 6 Comparison of the Hapke photometric parameters of asteroids *

Object	Type	ϖ (visible)	h	B_0	g	θ (°)	Reference
Average S		0.23	0.08	1.6	-0.27	20	Helfenstein and Veverka (1989)
Average C		0.037	0.025	1.03	-0.47	20	Helfenstein and Veverka (1989)
Average V (NEOs and Vesta)		0.51	0.098	1.0	-0.26	32	Hicks et al. (2014)
(4) Vesta	V	0.51	0.07	1.7	-0.24	18	Li et al. (2013a)
(951) Gaspra	S	0.36	0.06	1.63	-0.18	29	Helfenstein et al (1994)
(243) Ida	S	0.22	0.02	1.53	-0.33	18	Helfenstein et al (1996)
Dactyl	S	0.21	(0.020)	(1.53)	-0.33	23	Helfenstein et al. (1996)
(433) Eros	S	0.43	0.022	1.0	-0.29	28	Li et al. 2004
(25143) Itokawa	S	0.36	(0.022)	(1.0)	-0.51	(20)	Lederer et al. (2005)
(25143) Itokawa	S	0.42	0.01	0.87	-0.35	26	Kitazato et al. (2008)
(5535) Annefrank	S	0.41	0.015	1.32	-0.19	20	Hillier et al. (2011)
(1862) Apollo	S						Helfenstein and Veverka (1989)
(253) Mathilde	C	0.034	0.094	3.18	-0.27 (2-term fit)	25	Clark et al. (1999)
(1) Ceres	C	0.070	0.06	1.6	-0.4	44	Helfenstein and Veverka (1989); Li et al. (2006)
(2867) Šteins	E	0.57	0.062	0.60	-0.30	28	Spjuth et al. (2012)
(21) Lutetia	M	0.23	0.044	1.93	-0.25	25	Masoumzadeh et al. (2014)

* Values inside parentheses are assumed.

3.2. Itokawa

・測光をはやぶさ出発前に実施
単一散乱でのアルベド 0.36

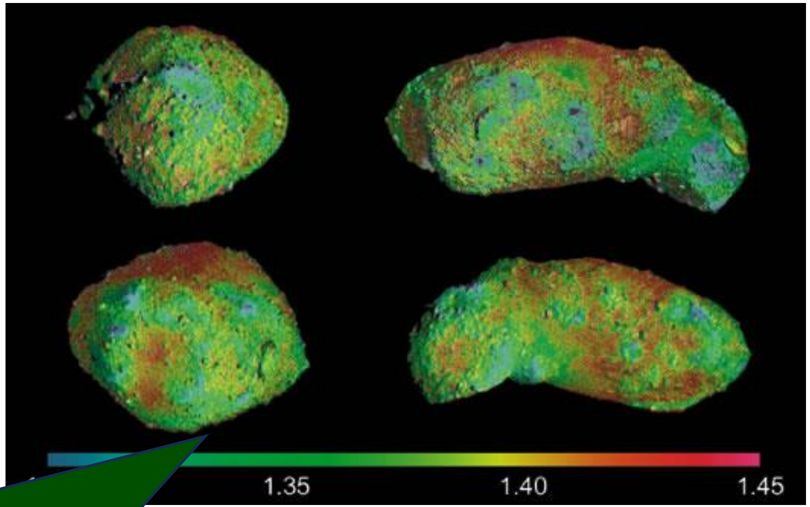

はやぶさ初号機によるローカルな測光観測結果
赤い部分は宇宙風化を受け古い地域、
青い部分はフレッシュな地域

Fig. 6. Local photometry image of Itokawa.

・はやぶさ初号機により0-38° で0.85-2.10 umでの分光
単一散乱でのアルベドは地上観測と一致
・低位相角でのデータから衝効果のモデル化が可能

3.3. Steins

- E-type
  単一散乱アルベド 0.57
  幾何アルベド 0.39,
  ボンドアルベド 0.24
  →E-typeの典型例と一致

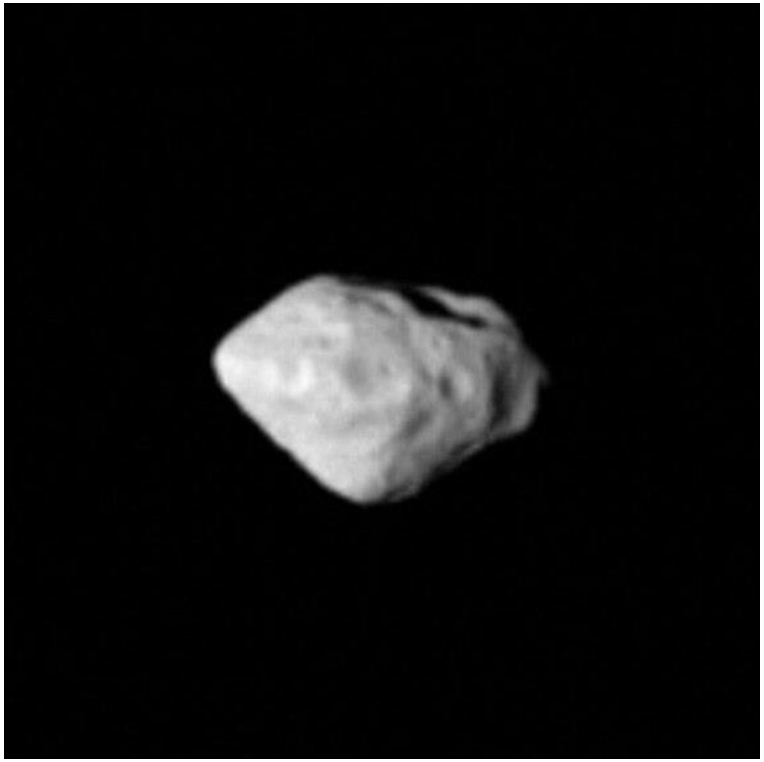

Fig. 7. Image of Steins.

- 高アルベドで強い衝効果
  レゴリスがポーラス（多孔質で高空隙率）の微粒子の特性と一致
  →実験室での結果と整合的

3.4. Lutetia

- 事前の地上観測ではC-typeと推定
- フライバイ観測ではM-typeで低空隙率
  →ラブルパイル（再集積体）ではない

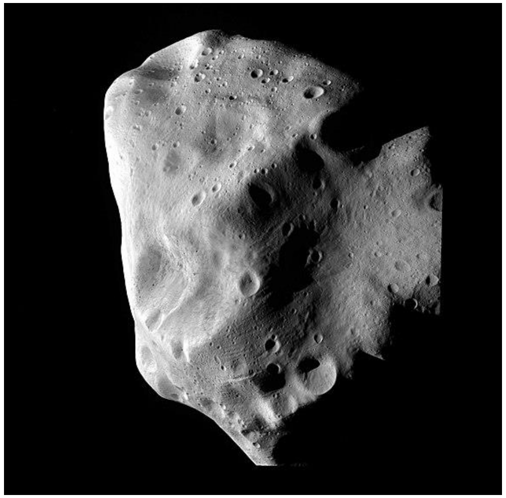

Fig. 8. Image of Lutetia.

Table 6 Comparison of the Hapke photometric parameters of asteroids *

Object	Type	ϖ (visible)	h	B_0	g	θ (°)	Reference
Average S		0.23	0.08	1.6	-0.27	20	Helfenstein and Veverka (1989)
Average C		0.037	0.025	1.03	-0.47	20	Helfenstein and Veverka (1989)
Average V (NEOs and Vesta)		0.51	0.098	1.0	-0.26	32	Hicks et al. (2014)
(4) Vesta	V	0.51	0.07	1.7	-0.24	18	Li et al. (2013a)
(951) Gaspra	S	0.36	0.06	1.63	-0.18	29	Helfenstein et al (1994)
(243) Ida	S	0.22	0.02	1.53	-0.33	18	Helfenstein et al (1996)
Dactyl	S	0.21	(0.020)	(1.53)	-0.33	23	Helfenstein et al. (1996)
(433) Eros	S	0.43	0.022	1.0	-0.29	28	Li et al. 2004
(25143) Itokawa	S	0.36	(0.022)	(1.0)	-0.51	(20)	Lederer et al. (2005)
(25143) Itokawa	S	0.42	0.01	0.87	-0.35	26	Kitazato et al. (2008)
(5535) Annefrank	S	0.41	0.015	1.32	-0.19	20	Hillier et al. (2011)
(1862) Apollo	S						Helfenstein and Veverka (1989)
(253) Mathilde	C	0.034	0.094	3.18	-0.27 (2-term fit)	25	Clark et al. (1999)
(1) Ceres	C	0.070	0.06	1.6	-0.4	44	Helfenstein and Veverka (1989); Li et al. (2006)
(2867) Šteins	E	0.57	0.062	0.60	-0.30	28	Spjuth et al. (2012)
(21) Lutetia	M	0.23	0.044	1.93	-0.25	25	Masoumzadeh et al. (2014)

* Values inside parentheses are assumed.

3.5. Vesta

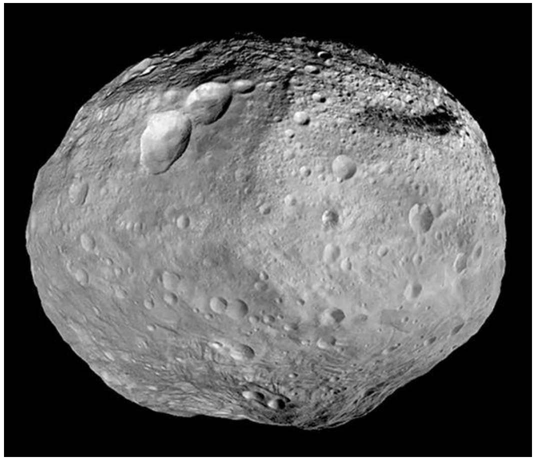

Fig. 9. Image of Vesta.

- V-type　特性はS-typeに似ているが、
  アルベドはS-typeの平均の2倍
- 表面不均一、衝突によるレゴリスの混合？

Table 6 Comparison of the Hapke photometric parameters of asteroids *

Object	Type	ϖ (visible)	h	B_0	g	θ (°)	Reference
Average S		0.23	0.08	1.6	-0.27	20	Helfenstein and Veverka (1989)
Average C		0.037	0.025	1.03	-0.47	20	Helfenstein and Veverka (1989)
Average V (NEOs and Vesta)		0.51	0.098	1.0	-0.26	32	Hicks et al. (2014)
(4) Vesta	V	0.51	0.07	1.7	-0.24	18	Li et al. (2013a)
(951) Gaspra	S	0.36	0.06	1.63	-0.18	29	Helfenstein et al (1994)
(243) Ida	S	0.22	0.02	1.53	-0.33	18	Helfenstein et al (1996)
Dactyl	S	0.21	(0.020)	(1.53)	-0.33	23	Helfenstein et al. (1996)
(433) Eros	S	0.43	0.022	1.0	-0.29	28	Li et al. 2004
(25143) Itokawa	S	0.36	(0.022)	(1.0)	-0.51	(20)	Lederer et al. (2005)
(25143) Itokawa	S	0.42	0.01	0.87	-0.35	26	Kitazato et al. (2008)
(5535) Annefrank	S	0.41	0.015	1.32	-0.19	20	Hillier et al. (2011)
(1862) Apollo	S						Helfenstein and Veverka (1989)
(253) Mathilde	C	0.034	0.094	3.18	-0.27 (2-term fit)	25	Clark et al. (1999)
(1) Ceres	C	0.070	0.06	1.6	-0.4	44	Helfenstein and Veverka (1989); Li et al. (2006)
(2867) Šteins	E	0.57	0.062	0.60	-0.30	28	Spjuth et al. (2012)
(21) Lutetia	M	0.23	0.044	1.93	-0.25	25	Masoumzadeh et al. (2014)

* Values inside parentheses are assumed.

3.6. Annefrank

- 単一散乱アルベド　0.62
  不規則形状→球形と仮定するとS-type
  と一致、単一散乱アルベド 0.41

Fig. 10. Image of Annefrank.

Table 6 Comparison of the Hapke photometric parameters of asteroids *

Object	Type	ϖ (visible)	h	B_0	g	θ (°)	Reference
Average S		0.23	0.08	1.6	-0.27	20	Helfenstein and Veverka (1989)
Average C		0.037	0.025	1.03	-0.47	20	Helfenstein and Veverka (1989)
Average V (NEOs and Vesta)		0.51	0.098	1.0	-0.26	32	Hicks et al. (2014)
(4) Vesta	V	0.51	0.07	1.7	-0.24	18	Li et al. (2013a)
(951) Gaspra	S	0.36	0.06	1.63	-0.18	29	Helfenstein et al (1994)
(243) Ida	S	0.22	0.02	1.53	-0.33	18	Helfenstein et al (1996)
Dactyl	S	0.21	(0.020)	(1.53)	-0.33	23	Helfenstein et al. (1996)
(433) Eros	S	0.43	0.022	1.0	-0.29	28	Li et al. 2004
(25143) Itokawa	S	0.36	(0.022)	(1.0)	-0.51	(20)	Lederer et al. (2005)
(25143) Itokawa	S	0.42	0.01	0.87	-0.35	26	Kitazato et al. (2008)
(5535) Annefrank	S	0.41	0.015	1.32	-0.19	20	Hillier et al. (2011)
(1862) Apollo	S						Helfenstein and Veverka (1989)
(253) Mathilde	C	0.034	0.094	3.18	-0.27 (2-term fit)	25	Clark et al. (1999)
(1) Ceres	C	0.070	0.06	1.6	-0.4	44	Helfenstein and Veverka (1989); Li et al. (2006)
(2867) Šteins	E	0.57	0.062	0.60	-0.30	28	Spjuth et al. (2012)
(21) Lutetia	M	0.23	0.044	1.93	-0.25	25	Masoumzadeh et al. (2014)

* Values inside parentheses are assumed.

4.1. Correction for spectral analysis

・小惑星表面の反射率の変動補正
　低アルベド　多重散乱を無視できる
　高アルベド、表面不均一　補正が困難

・フェイズレッドニング
　S-typeで顕著、
　C-, E-typeでは影響が少ない
　→高アルベドなほど、
　　多重散乱光が増加し赤く

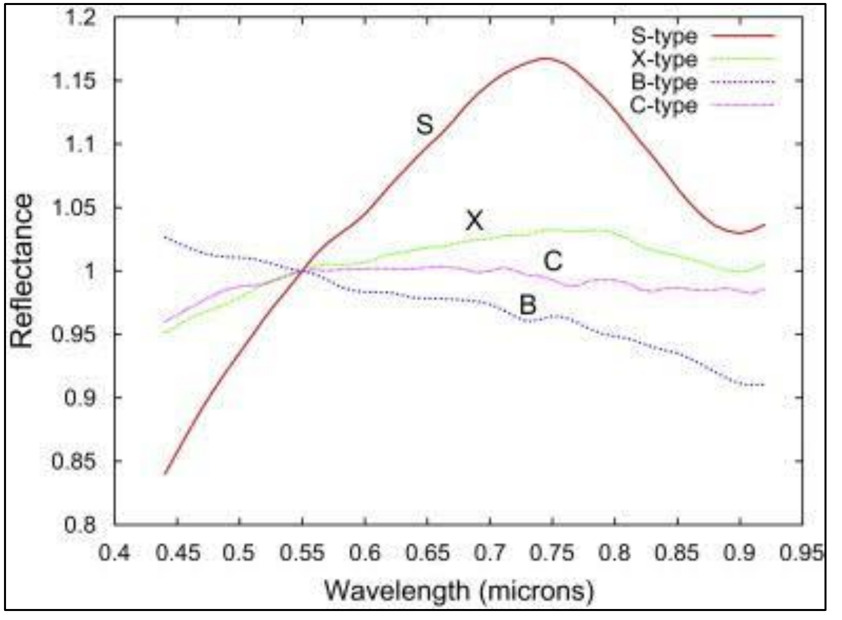

Fig. 11. Reflectance spectral of each type asteroids.

4.2. Taxonomic classes

- Q-type　S-typeに似ているがアルベドが高く、表面がフレッシュ（宇宙風化されていない）
- NEAsはMBAsに比べ宇宙風化が進んでいないQ-typeが多い→隕石

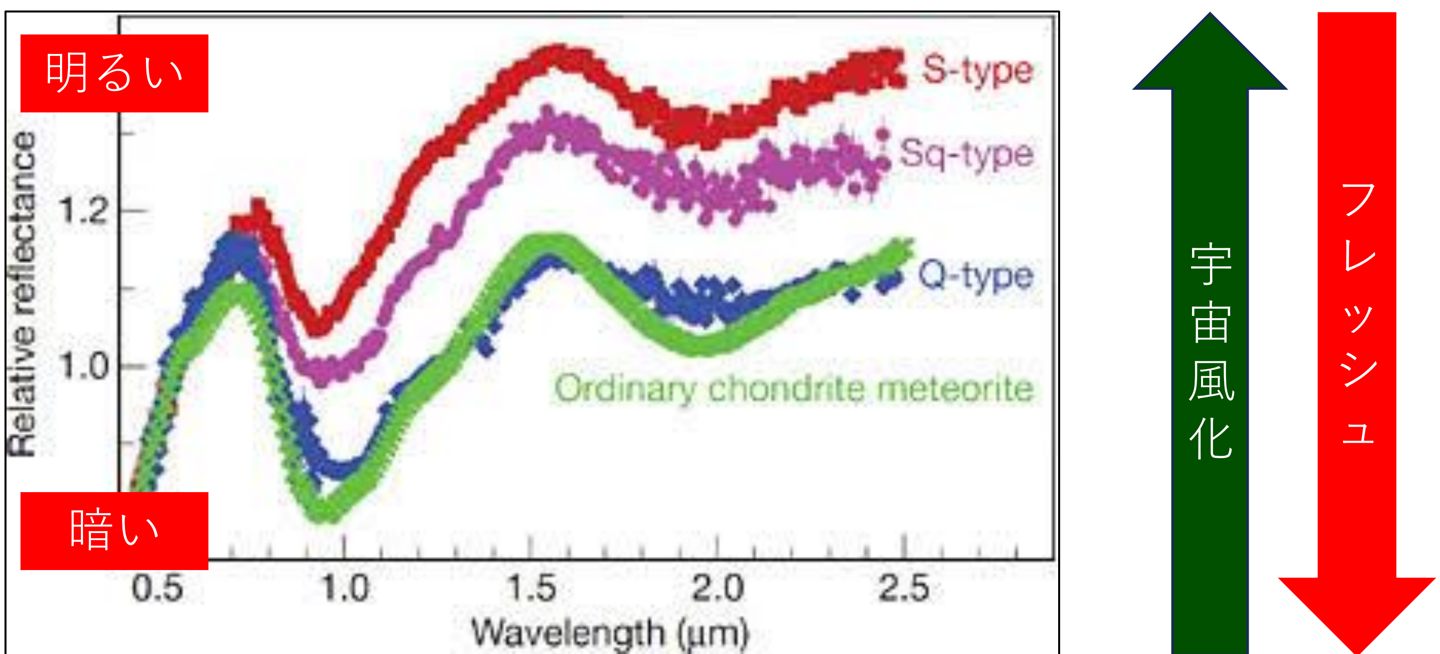

Fig. 12. Reflectance spectral of S-, Sq-, Q-type asteroids.

4.3. Context of geological process

・クレーター　衝突の履歴、長期間
　滑らかな地形　火山活動、最近の再表面化
　低ラフネス　デブリフロー、堆積現象

・質量が大きいと微粒子が（重力で）保持、低ラフネス

・レゴリスの多孔質、圧縮状態は微粒子の衝突、堆積
　など多様なプロセスで変化していく
　→モデルの限界

5. SUMMARY AND FUTURE PERSPECTIVE

・測光観測によるモデリングの重要性
1. 表面特性　2. 測光補正　3. その場観測サポート
・Hapkeモデルの進展
SHOEとCBOEの理解を深める試み
・探査機のその場観測は表面の理解を深めるために重要

・広い位相角での測光観測データの取得
メインベルト、地球近傍小惑星
・探査機、実験室、地上観測データの統合
Hapkeモデルの向上へ